First experimental Investigations on Dynamic Aeroelastic Stability of Panels in the Transonic Domain at the German Aerospace Center (DLR)

J. Lübker*

DLR, German Aerospace Center, Göttingen, 37073, Germany

M. Alder†

DLR, German Aerospace Center, Braunschweig, 38108, Germany

H. Fink‡

DLR, German Aerospace Center, Göttingen, 37073, Germany

An forced motion experiment on earoelastic stability is performed within a Mach number domain of $0.7 < M < 1.2$. The panel structure is deflected in its first bending mode shape. The objective is to obtain the aerodynamic response over an extensive range of amplitudes and frequencies of panel motions. Beside the measurement of the panel deformation by a stereo camera marker tracking system, the flow response is measured by high sensitive miniature pressure transducers. Results of pressure coefficient distribution measurements and deformation measurements are presented. Concluding, first preliminary comparisons of experimental data and numerical results gained within the project are are discussed.

Nomenclature

$\hat{A}$	Deflection amplitude, mm
a	Panel length, mm
b	Panel width, mm
c_p	Pressure coefficient: $(p - p_\infty)/q_\infty$
D	Plate Stiffness
F	Force, N
f	Excitation frequency, Hz
h	Panel thickness, mm
k	Reduced excitation frequency: $fa2\pi/u_\infty$
M	Mach number
N	Number of sensors along the panel length a
p	Pressure, Pa
q	Dynamic pressure, Pa
Re	Reynolds number
T	Time of oscillation, s
t	Time, s
W^*	Work equivalent: $c_p dz/\hat{A}^2$
x, y, z	Cartesian coordinates
α	Angle , °

*PhD Student, DLR Institute of Aeroelasticity, Bunsenstraße 10, 37073, Göttingen, jannis.luebker@dlr.de.

†PhD Student, DLR Institute of Aerodynamics and Flow Technology, Lilienhalplatz 7, 38108, Braunschweig, marko.alder@dlr.de.

‡Design Engineer, DLR Systemhaus Technik, Bunsenstraße 10, 37073, Göttingen, helena.fink@dlr.de.

δ_{99} Boundary layer thickness
λ $\lambda^*/\sqrt{M^2-1}$
λ^* Nondimensional dynamic pressure: $\rho_\infty u_\infty^2 a^3/D$
μ Mass ratio: $\rho_{fluid} a/\rho_{structure} h$
ω Circular frequency, 1/s
ϕ Phase angle, $^\circ$
ρ Density, kg/m^3

Subscript
0 Total physical quantity
crit Critical value
i Variable number
N Normalized value
∞ Related to freestream conditions

I. Introduction

The aeroelastic stability of plates has first been observed in the 1940's because self-excited oscillations of aerodynamic skin panels threatened the structural integrity of the first rockets and high performance aircraft.[1] As a consequence numerous theoretical and experimental studies on static and dynamic instabilities of plates and shells followed in the 1960's and 70's. Comprehensive reviews are given by Dowell[2,3] and Johns.[4] It is well established on experimental grounds that panels which are restrained at all edges, such as skin panels in monocoque structures, exhibit dynamic instabilities in supersonic flow. Muhlstein et al.[5] and Gaspers et al.[6] not only observe that the critical dynamic pressure for flutter onset (in non-dimensional form referred to as λ_{crit}) drastically decreases at low supersonic Mach numbers, but also confirm that a fluid boundary layer significantly increases the aerodynamic damping, which in return attenuates the first effect (see Fig. 2 (a)). These results encouraged theoretical studies to include viscous flow effects in panel flutter computations. Early studies basically apply linearized potential flow aerodynamics extended by an explicit definition of a nonuniform mean flow[7,8] or a one-seventh power law for the mean velocity distribution in a turbulent boundary layer.[9,10] More recent studies account for viscous flow effects by solving Reynolds-averaged Navier-Stokes (URANS) equations.[11–13]

A representative result of such studies is shown in figure 1(a) for a two-dimensional flat plate (adapted from[13]). It is shown with respect to a trajectory of a Saturn V launch vehicle[14] that the low supersonic Mach numbers are most critical in terms of preventing dynamic-instabilities. Two different types of flutter may occur. A typical mechanism leading to self-excited oscillations is the coalescence of the lowest eigenmodes (called coupled-mode flutter). However, at low supersonic Mach numbers flutter may also occur due to negative aerodynamic damping in a single generalized coordinate, which is thus referred to as single-mode flutter. Prior experiments basically focus on a determination of λ_{crit}[5,6,15] over a wide range of Mach numbers M and dynamic pressures λ. Thus, the parameter space which needs to be considered in such experimental stability studies is large, including numerous geometrical and material properties of the structural model which sensitively affect the aeroelastic response. In order to achieve a better understanding of panel flutter phenomena, such as single-mode flutter and the influence of a boundary layer, an experimental test environment is designed to measure the aerodynamic response on forced oscillations of a rectangular plate in its generalized coordinates. As opposed to Muhlstein,[16] who determined λ_{crit} by evaluating the mechanical impedance of a forced-motion system, the present test setup is designed well below the flutter boundary in order to focus the aeroelastic response in terms of amplitude and phase of the plate surface pressure. On the one hand, this allows for a determination of generalized aerodynamic forces to analyze the aeroelastic stability based on small perturbation theory in the frequency domain. But it furthermore allows, in the framework of single-mode flutter, to study the physical mechanism of negative aerodynamic damping by applying the energy method, because the lowest eigenmode is weakly influenced by aerodynamic coupling effects (see Fig. 2 (b)).

The present paper presents some results of a test campaign in the Transonic Wind Tunnel in Göttingen (DNW-TWG) for a Mach number range of $0.7 \leq M \leq 1.2$ and reduced frequency range of $0 < k < 0.7$. The first part is devoted to a description of the test setup, followed by the identification of aerodynamic forces. This includes measurements of the underlying structural deformations in order to assess the error in

excitation of the first panel mode shape. By applying a Fourier transform, the measured aerodynamic data is filtered and expressed as pressure coefficient c_p, which is further analyzed with respect to its dependence on the structural deflection amplitude. Finally the results compared to the numerical data computed within the project by means of absolute values and phase angles.

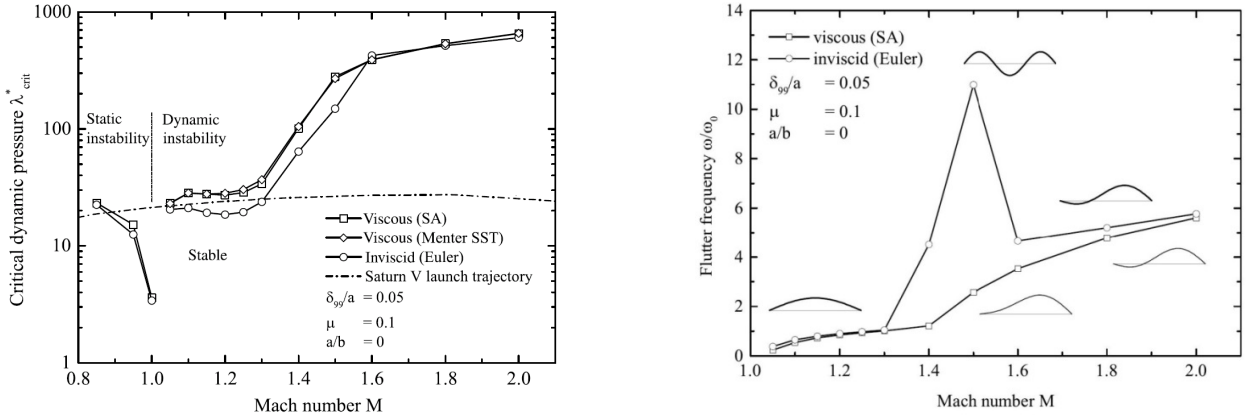

(a) Aeroelastic stability boundary.[13]

(b) Instability frequencies and shapes.[13]

Figure 1. 2D numerical results for aeroelastic instabilities in the transonic domain

II. Numerical Setup

The experimental activities are accompanied by 2D and 3D coupled CFD/FE calculations. Since the introduction (figure 1) as well as the later on discussed test setup design and the comparison of the results at the end of this report refer to the numerical results a brief description of the numerical computations is given. For the 2D as well as for the 3D calculations the structural solver MSC NASTRAN is used. The DLR-TAU code is used in both cases for solving the compressible three-dimensional Navier-Stokes and the Euler equations. The computational domains (2D and 3D) used are illustrated in figure 2 (a). The structural model is a flat rectangular plate, which is build up of 100 x 200 CQUAD4 elements. Just as the experimental setup the aspect ratio of the numerical structure is a/b and clamped mechanical boundary conditions act on all four edges. Only one surface of the panel is exposed to the flow. A detailed explanation of the used coupled calculations environment can be looked up in Alder.[13] The calculations referred to in the introduction are done in the 2D domain with $a/b = 0$ (figure 1). The deflection shape of the numerical forced motion investigations, which are discussed in the final section of this report, is the first mode shape of a flat plate with clamped mechanical boundary conditions at all four edges (figure 2 (b)).

III. Test Setup and Test Procedure

The test setup was designed and manufactured to provide a new experimental environment for wind tunnel panel flutter tests. Prior experiments often focused on the whole aeroelastic system, which means the aerodynamic loads as well as the structural system. By conducting a forced motion experiment most structural parameters can be neglected. The objective is the investigation of the aerodynamic response to the structure's motion. By identifying responses over a certain range of frequencies the transfer function can be determined. In the first experiments a model with basic characteristics is investigated, which simplify the corresponding numerical simulations as well as the analysis of the gained test results. A flat plate with clamped mechanical boundary conditions for all four edges is implemented in the wind tunnel's wall in such a way, that one surface of the panel is exposed to the flow. Results concerning aeroelastic stability of a 2D simply supported panel are shown in figure 1 (b). The panel model used here is a flat plate with one surface exposed to the flow. The flutter frequency is plotted against the Mach number. Viscous and inviscid results are presented. The domain which is crucial for the later on described experiments is in between $1.0 < M < 1.2$. Viscous and inviscid solutions differ very slightly here. Crucial for the considerations concerning the experimental design are the sketched flutter shapes, which are to be expected. In the region of interest the shape is highly dominated by the panel's first bending mode shape. Referring to that one

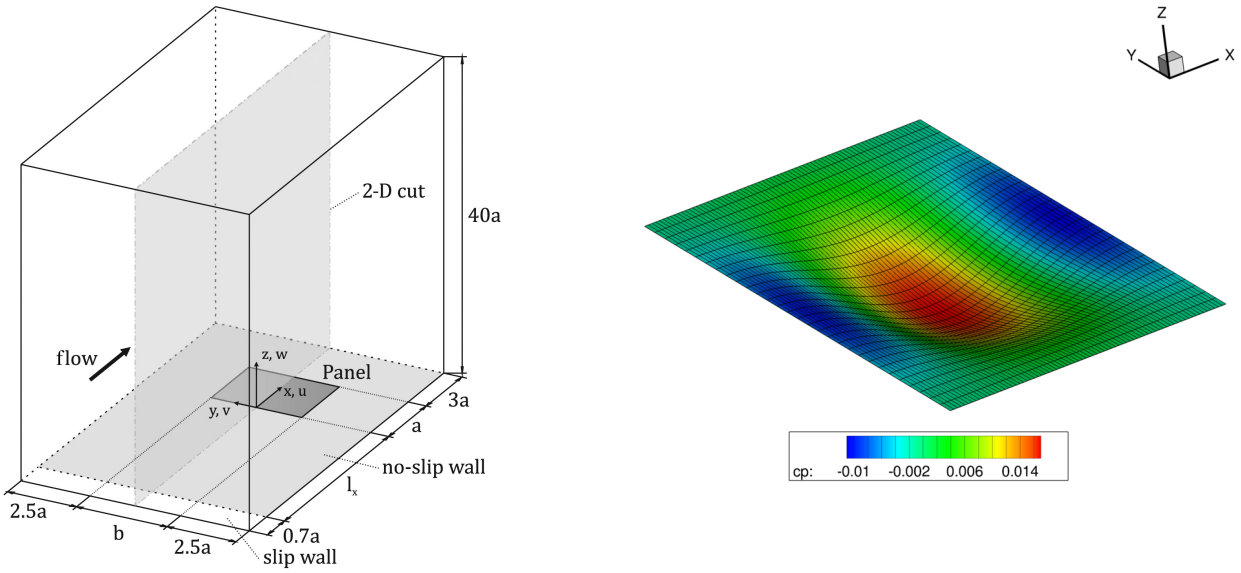

(a) Computational domains.[13]

(b) Clamped plate's first mode shape.

Figure 2. Numerical setup.

speaks of single mode flutter. That does not mean that there is no contribution of the second bending mode shape at all. It is well known that panels with clamped mechanical boundary conditions and simply supported panels show equal behaviors (neglecting the offset in critical dynamic pressure) concerning their aeroelastic stability. The obtained shape is chosen to be the design shape which is to be simulated in the experimental forced motion activities at hand. For the deflection of the panel in the form of the corresponding modeshape an actuator is placed behind the panel's rear side. The hydraulic cylinder with its point of application in the panel's center deflects the panel in a wide frequency range for different amplitudes. The whole test setup, which is to be mounted to the wind tunnel, is shown in Fig. 3. The Panel Assembly consisting of the actual panel within another massive steel frame is mounted to another support structure, the so-called Inner Frame. This structure carries as well the mounting rack of the actuator. This assembly is then again mounted to the Outer Frame which connects the setup to the wind tunnel.

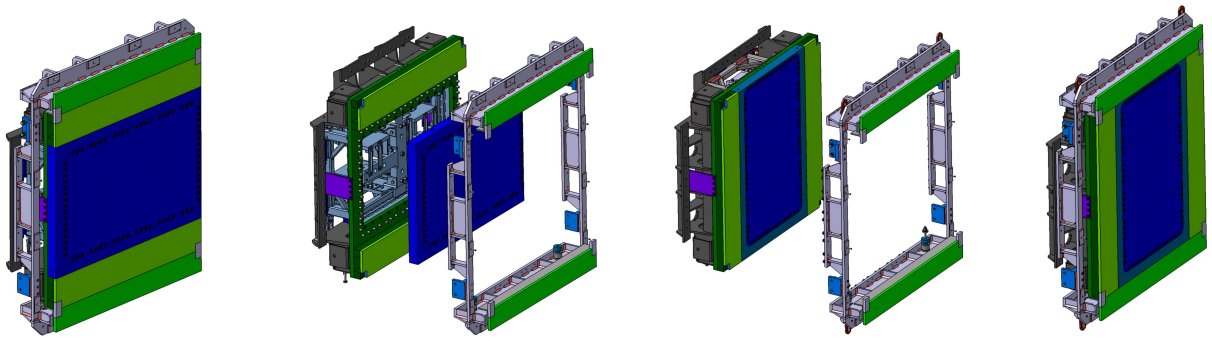

(a) (b) (c) (d)

Figure 3. Panel flutter test setup (a)**, Exploded assembly drawing (Setup configuration** $\alpha_0 = 0°$**)** (b) **, Setup configuration** $\alpha_1 = 90°$ (c) & (d)**.**

The described complex design of the test setup is based on the idea of being able to do investigations on numerous parameters that influence panel flutter. The resulting modular design provides possibilities to integrate panels of different materials, sizes, curvatures and mechanical boundary conditions. Furthermore the actuator rack can be removed to perform free flutter experiments or it can be exchanged for a pressure chamber to conduct experiments on cavity effects. Since the Inner Frame can be rotated 90 degrees, tests on different panel aspect ratios are possible by using the same panel (figure 3 (a), (d)). In order to implement different deflection shapes the mentioned actuator rack provides mounting slots for different

actuator configurations. The panel (figure 4) is equipped extensively with measurement technique. Its dimensions are $a = 500$mm in streamwise, respectively x, direction and $b = 875$mm in crossstreamwise, respectively y, direction. In order to measure the transfer behaviour of the aeroelastic system, measurement techniques for the deformation in z direction and for the pressure distribution p are applied. The deformation measurement technique is a stereo camera based marker tracking system, the so-called PicColor system. Two cameras in a certain angle to the perpendicular line of the panel surface are recording a pattern of markers applied to the panel's surface (figure 4 (a), (b)). The cameras are positioned outside the test section behind a window opposite to the panel. The aerodynamic loads are measured by means of 108 high sensitive unsteady pressure transducers. Those are arranged in a way similar to the PicColor marker pattern. Owing to the impact of the turbulent boundary layer a wake rake equipped with 64 pitot tubes along a vertical distance of 100 mm is mounted downstream of the panel. Figure 4 (b) shows a view from inside the test section in flow direction. The panel is part of the test section's side wall. The boundary layer rake as well as the marker pattern and the perforated walls of the used Perforated Test Section are visible. A detailed survey on the setup's design and its instrumentation is available in Lübker et al.[17]

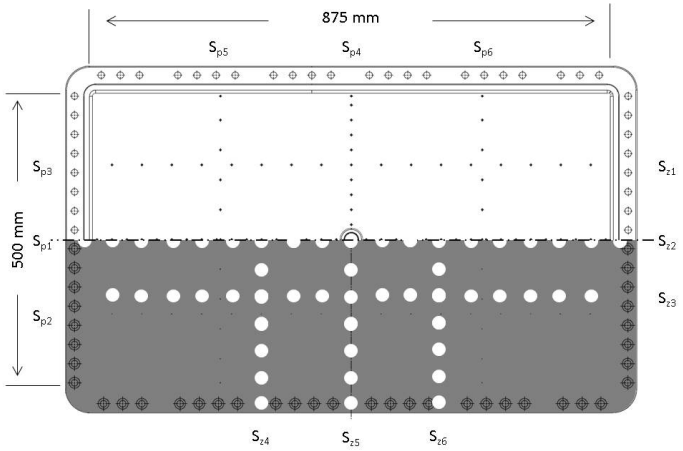

(a) Top view of the panel (bottom) with PicColor marker pattern and rear side of the panel with pressure transducer positions (top).

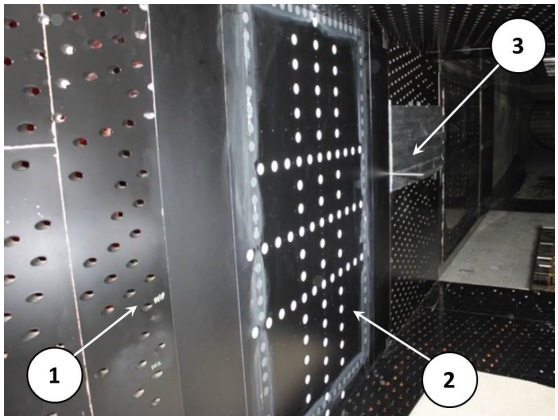

(b) View in direction of flow. Perforated wall steel sheets (1); Panel with marker pattern (2); Boundary layer rake (3).

Figure 4. Panel model.

The experiments were conducted in the Transonic Wind Tunnel Gttingen (DNW-TWG), which is a closed return type wind tunnel. It allows conducting the panel flutter tests for a Mach number range in between $0.7 < M < 1.2$. The 1m by 1m test section is surrounded by a pressure chamber, which offers a variation of the total pressure in a range within approximately 35kPa $< p_0 <$ 135kPa. The Mach number range was divided into steps of $\Delta M = 0.05$ for a proper resolution. The total pressure level varied within 0.3bar$< p_0 <$ 0.4bar, which led to a low level of aerodynamic loads interacting with the panel. The Reynolds number was constant at $Re = 2.5E+06$. In each measurement point a variation of the excitation frequency f and the amplitude $\hat{A}$ ($\hat{A}_1 = 0.6$mm, $\hat{A}_2 = 1.2$mm and $\hat{A}_3 = 1.8$mm) of the panel's center deflection was investigated. Table 1 and table 2 show in brief the investigated flow parameters and the model parameters.

Table 1. Flow Parameters

Parameter	Min.	Max.
$M_\infty, [-]$	0.7	1.2
$p_0, [kPa]$	34.8	42.0

Table 2. Model Parameters

Parameter	Min.	Max.
$k, [-]$	0.0	0.7
$\hat{A}, [mm]$	0.6	1.8

IV. Results

The results of displacement measurements and pressure distribution measurements are presented for zhe centerline of the panel for four examplary measurement points. The belonging sensor positions are along the the S_{z5} line related to the deformation measurement and the S_{p4} line related to the pressure measurements

(figure 4 (a)). The results are shown for a low Mach number at subsonic conditions and for a high Mach number at supersonic conditions. In each of those Mach numbers a low excitation frequency as well as a high excitation frequency is presented.

IV.A. Displacements

A comparison of the measured panel deflection and the design shape is depicted in figure 5. The x axis is normalized by the panel's length a. The z axis is divided by the nominal deflection amplitude. The black dashed line illustrates the first bending mode design shape for comparison with the measured shape. Beside the design shape the totality of results of the measured time steps of one oscillation period are represented by the grey domain. Eight particular chosen examplary time steps, depicted in white, show the actually measured deformation shapes. In case of the low excitation frequency a very agreement between intended shape and measured shape is recognizable. With increasing frequency slight deviations of the measured amplitude occur. Nevertheless the general agreement of the shapes is still very good. This observation is valid for the subsonic and the supersonic examples. As discussed later on those deviations are non-relevant. Within the presented parameter range neither the Mach number nor the excitation frequency is affecting the resulting shape in a serious way.

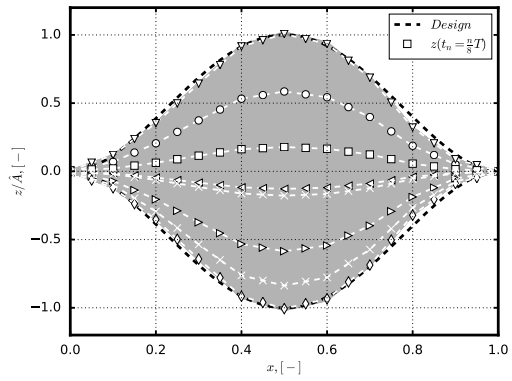

(a) $M = 0.7; k = 0.12; \hat{A} = 1.8mm$

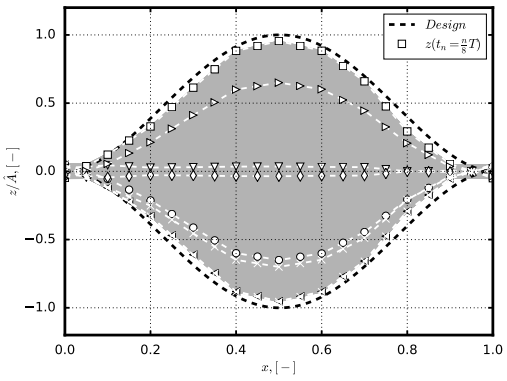

(b) $M = 0.7; k = 0.71; \hat{A} = 1.8mm$

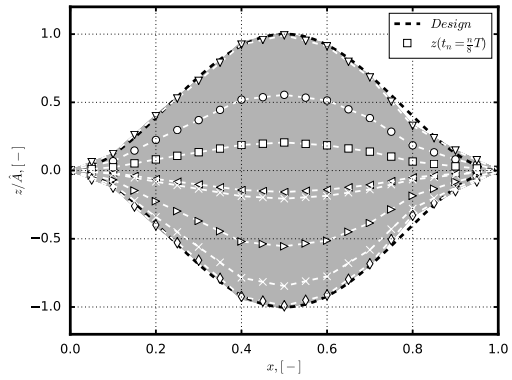

(c) $M = 1.15; k = 0.07; \hat{A} = 1.8mm$

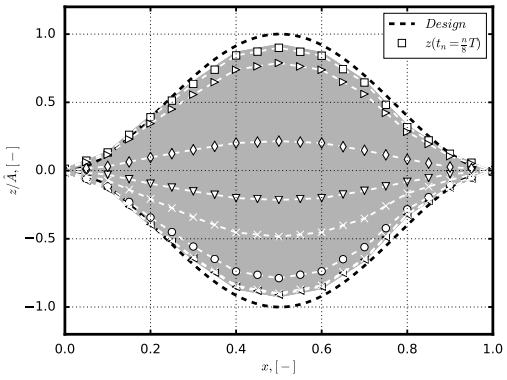

(d) $M = 1.15; k = 0.51; \hat{A} = 1.8mm$

Figure 5. Deformation (abs. values) for different excitation frequencies and Mach numbers.

Parts of the panel, which are not close to the edges or to the deflection mechanism at its centre are without defined mechanical bounday conditions. It is considered possible that those parts' oscillations show a phase shift compared to the motion of the panel's deflection mechanism. With respect to the intended ideal mode one deformation a phase shift of $\phi = 0°$ is wanted. The calculated phase angles, which are related to the panel deflection mechanism, show values close to $\phi = 0°$ (figure 6). Exceptions are recognizable for all four examples at the leading edge end the trailing edge. The phase shift may be due to measurement uncertainties. Either way the phase shifts are considered negligible. The amplitudes at the edges are about

$\hat{A} = 0$mm and close to the edges still very small. For that reason an influence on further calculations is not to be expected.

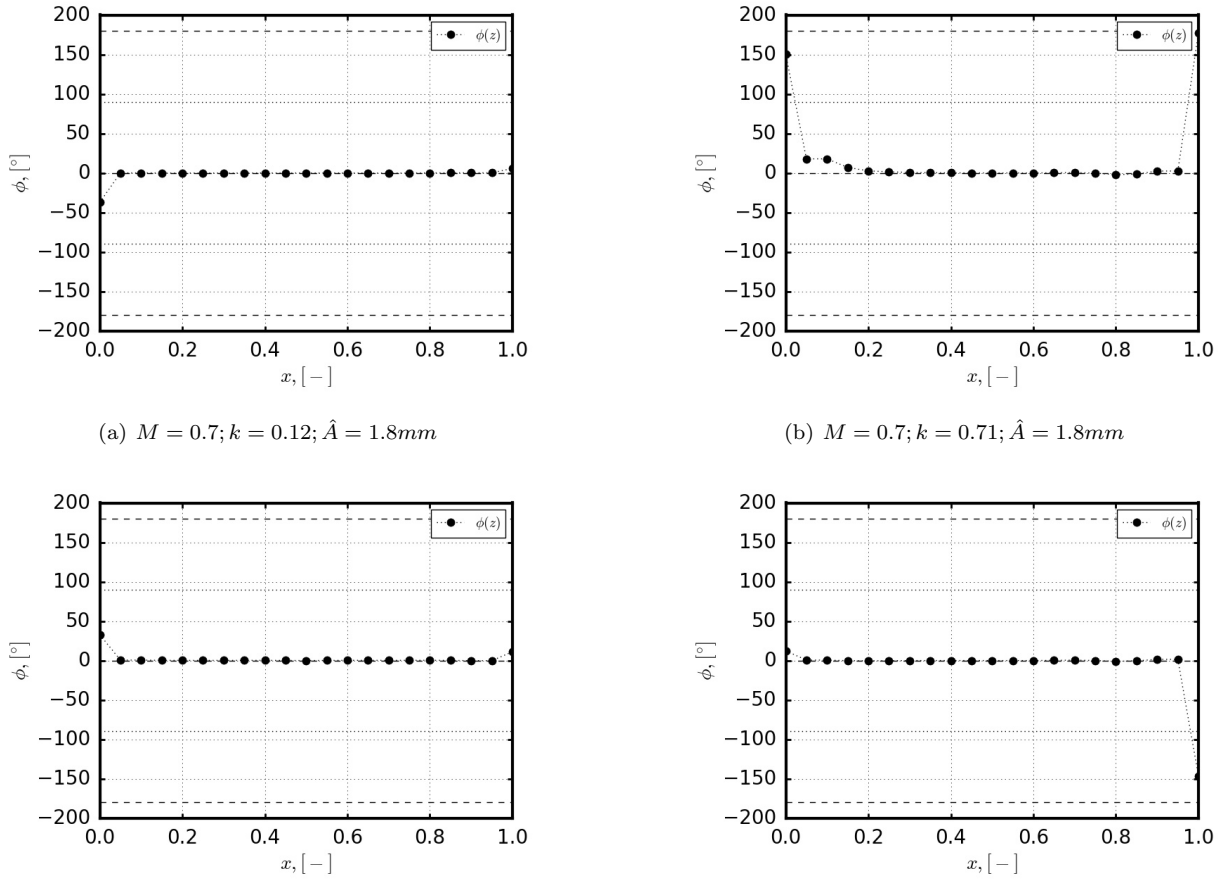

(a) $M = 0.7; k = 0.12; \hat{A} = 1.8mm$

(b) $M = 0.7; k = 0.71; \hat{A} = 1.8mm$

(c) $M = 1.15; k = 0.07; \hat{A} = 1.8mm$

(d) $M = 1.15; k = 0.51; \hat{A} = 1.8mm$

Figure 6. Deformation (phase angles) for different excitation frequencies and Mach numbers.

IV.B. Pressure Coefficients

Results of the same measurement points as presented for the deflections are shown in figure 7 and figure 8 for the pressure measurements. Apart from a depicted design shape the illustrations are done in the same way as before. The pressure coefficient is divided by the excitation amplitude. Three domains are recognizable which oscillate in phase opposition. At low excitation frequencies the different domains are divided by zero points located at the inflexion points of the deflected panel. A standing wave is established here (figure 7 (a), (c)). With increasing excitation frequency the characteristic changes by adding characteristics of a traveling wave (figure 7 (b), (d)). The zero points disappear more and more by increasing excitation frequency. The shape of the measured pressure distribution is changing by comparison of the subsonic case and the supersonic case. For the low Mach number the shape is vertical symmetric related to the y axis at $x = 0.5$. With increasing Mach number the oscillation at the leading edge is strongly increased in amplitude and spatial extent along the x axis. The trailing edge oscillation is changed in the opposite way. With increasing excitation frequency the measured pressure maximum is slightly increasing at the subsonic Mach numbers and slightly decreasing for the supersonic Mach numbers. In contrast to the deflection shapes the pressure coefficientsdistributions are strongly influenced by both the Mach number and the excitation frequency.

The phase angles illustrate the mentioned behaviour (figure 8 (a)). Two zero degrees phase shift areas show the oscillations at leading edge and trailing edge. The 180 degrees area in between shows the oscillation at the panel's centre area. The very sharp transition between the areas in the low frequency cases gives way to a softened transition at high frequencies. This softening correlates with the afore mentioned vanishing of

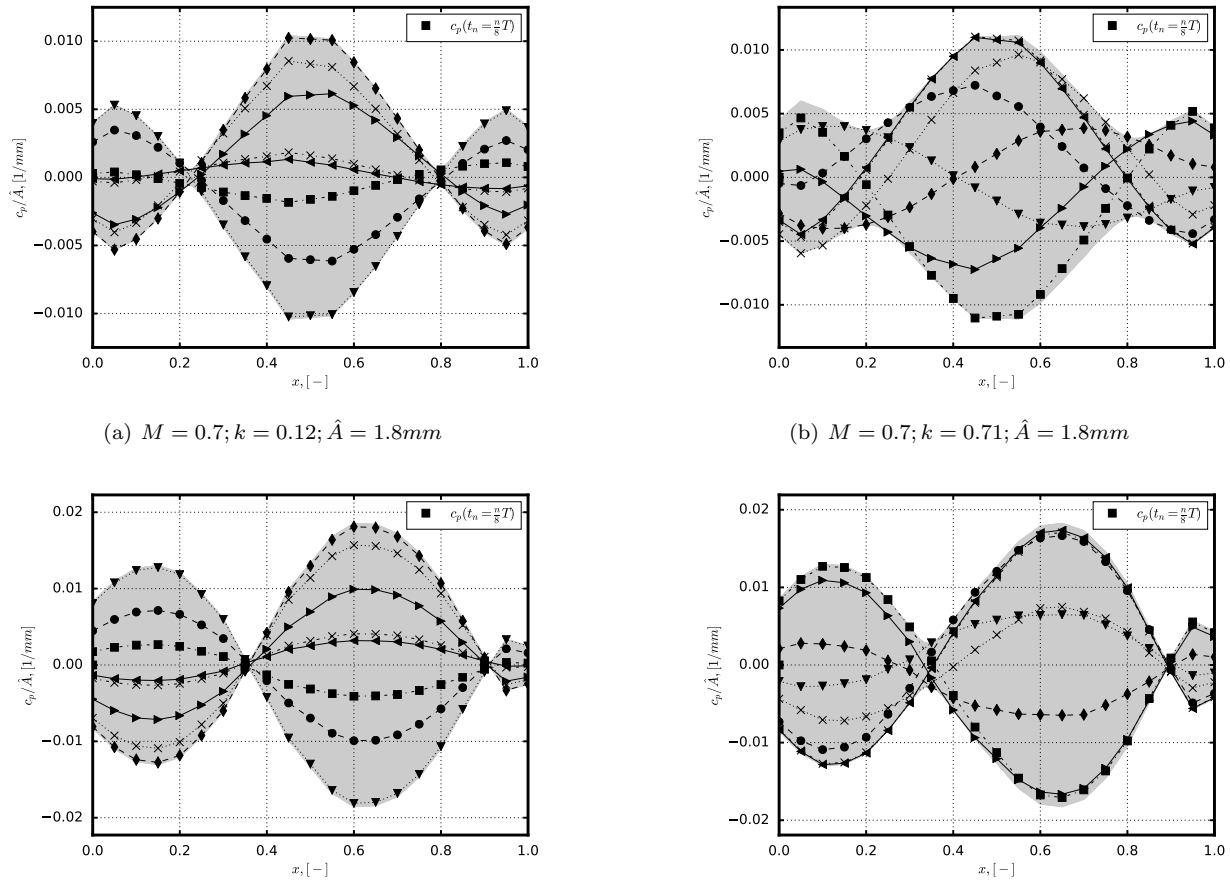

(a) $M = 0.7; k = 0.12; \hat{A} = 1.8mm$

(b) $M = 0.7; k = 0.71; \hat{A} = 1.8mm$

(c) $M = 1.15; k = 0.07; \hat{A} = 1.8mm$

(d) $M = 1.15; k = 0.51; \hat{A} = 1.8mm$

Figure 7. Pressure distributions (absolute values) for different excitation frequencies and Mach numbers.

the zero points. By comparison of the subsonic cases to the supersonic cases the shift of the zero points in streamwise direction is obvious.

Having a closer look at the amplitude measuring results of single pressure transducers are compared for the tested different excitation amplitudes in figure 9. Due to the necessary phase shift for this kind of data presentaion different pressure transducer positions are chosen. One period of pressure coefficient oscillation is plotted against one period of actuator oscillation. Both are reduced by the particular excitation amplitude. The agreement of all three datasets is convincing and shows a strongly linear dependency of the pressure amplitude on the deflection amplitude. That means for the further analysis that by reducing the deflections as well as the pressure measurements triple data sets for all variations of Mach number and excitation frequency are available. It shows further that the decrease in achieved panel deflection at high Mach numbers can be equalized.

IV.C. Experiment versus numerical data

Apart from the density of sensor positions along the panel's length the results of the absolute values of the normalized pressure measurements are in good agreement with each other. The three oscillation areas are clear as well as the zero points at low frequencies and their vanishing at high freqiencies (figure 10). Nevertheless, discrepancies emerge in particular in the vicinity of leading edge and trailing egde. The discrepancies are in clearly by having a look at the results at the high Mach number and high excitation frequency example.

The illustrated experimental and numerical phase angels show good compliance as well (figure 11). The domains of zero degrees phase shift and 180 degrees phase shift are very clear. Both results show the softening effect for both Mach numbers with increasing excitation frequency. Both results show the streamwise shift

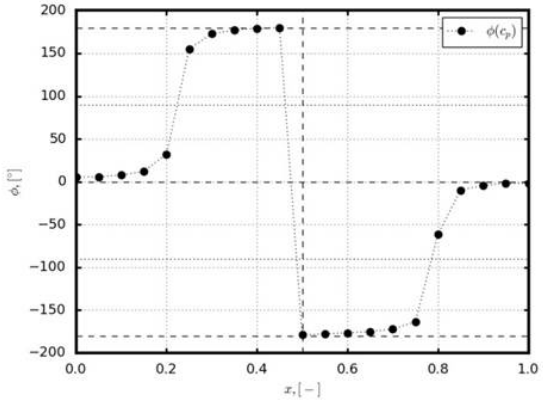

(a) $M = 0.7; k = 0.12; \hat{A} = 1.8mm$

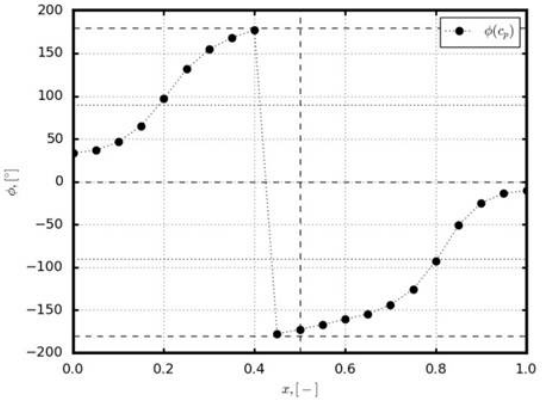

(b) $M = 0.7; k = 0.71; \hat{A} = 1.8mm$

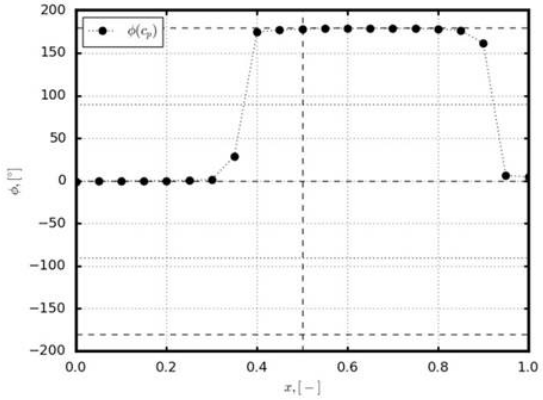

(c) $M = 1.15; k = 0.07; \hat{A} = 1.8mm$

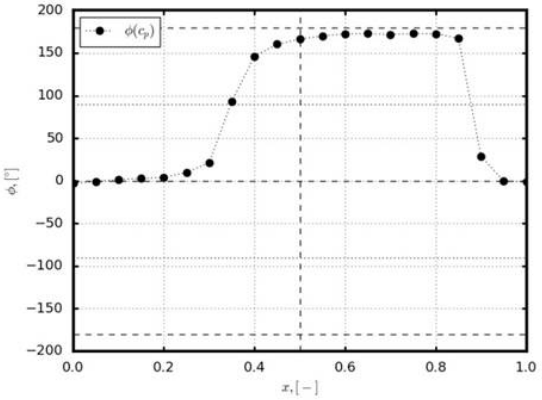

(d) $M = 1.15; k = 0.51; \hat{A} = 1.8mm$

Figure 8. Pressure distributions (phase angles) for different excitation frequencies and Mach numbers.

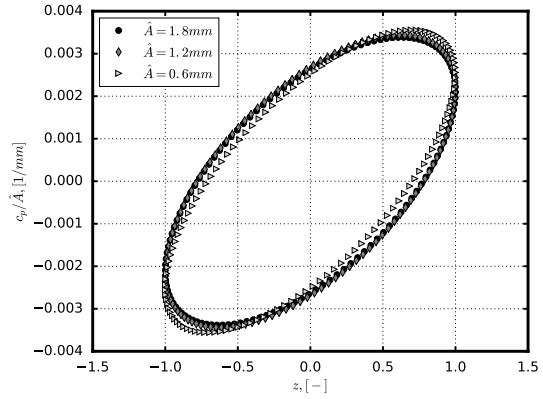

(a) $M = 0.7; k = 0.71$

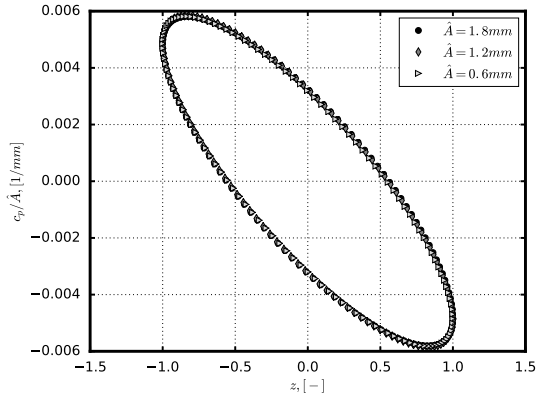

(b) $M = 1.15; k = 0.51$

Figure 9. Comparison of normalized pressure coefficients results for all three tested excitation amplitudes.

of the transition for high Mach numbers. Differences occur at the locations of the transition for the low frequency cases in particular at the trailing edge. In case of the supersonic examples one special discrepancy is striking. The numerical results are increasing steadily along the panel's length. The measured phase angles are increasing until a decrease occurs at about $x = 0.9$. Both behaviours result finally again in a phase angle of zero.

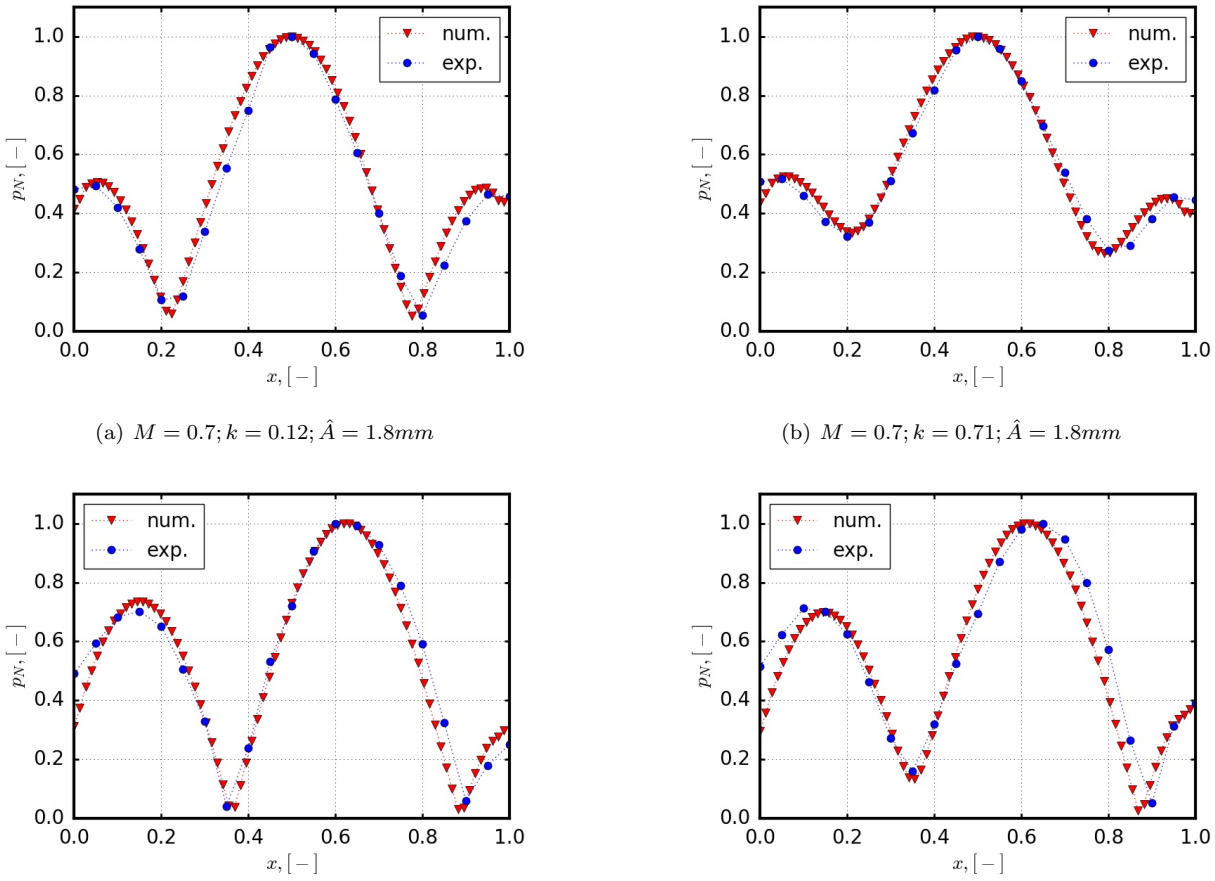

(a) $M = 0.7; k = 0.12; \hat{A} = 1.8mm$

(b) $M = 0.7; k = 0.71; \hat{A} = 1.8mm$

(c) $M = 1.15; k = 0.07; \hat{A} = 1.8mm$

(d) $M = 1.15; k = 0.51; \hat{A} = 1.8mm$

Figure 10. Pressure distribution, Comparison of absolute values.

V. Conclusions

A flat rectangular panel is investigated in the transonic Mach number domain. The displacements of a first bending mode were forced by means of a hydraulic system. The objective was the measurement and the analysis of the aerodynamic response measured by high sensitive dynamic pressure transducers. Experimental requirements and the derived test setup design were desribed. The measured data of deflection measurements and pressure measurements were presented. The deflection data showed a good agreement with the intended design shape related to absolute values and phase angles. The influence of Mach number and excitation frequency on the pressure distribution was discussed.
Although the preliminary comparisons of experimental data and results of coupled 3D CFD/FE calculations showed good agreements, discrepancies in absolute values and phase angles occured. With respect to the aeroelastic stability a serious considerations of the phase angles are necessary. The angles and the imaginary parts of the aerodynamic responses give information about the carried out work between structure and fluid. According to that a drop of the phase angle instead of an increase may lead to a change of the algebraic sign and consequently to a strongly different result. The carried out numerical forced motion investigations used a ideal mode one mode shape of a flat plate. Among other reasons the slight differences in experimental and numerical excitation shapes may lead to the observed differences.

VI. Outlook

In spite of the good agreement between numerical and experimental data sets discrepancies were evident. Further comparisons are necessary. Based on the measurements of pressure distribution and panel deflection

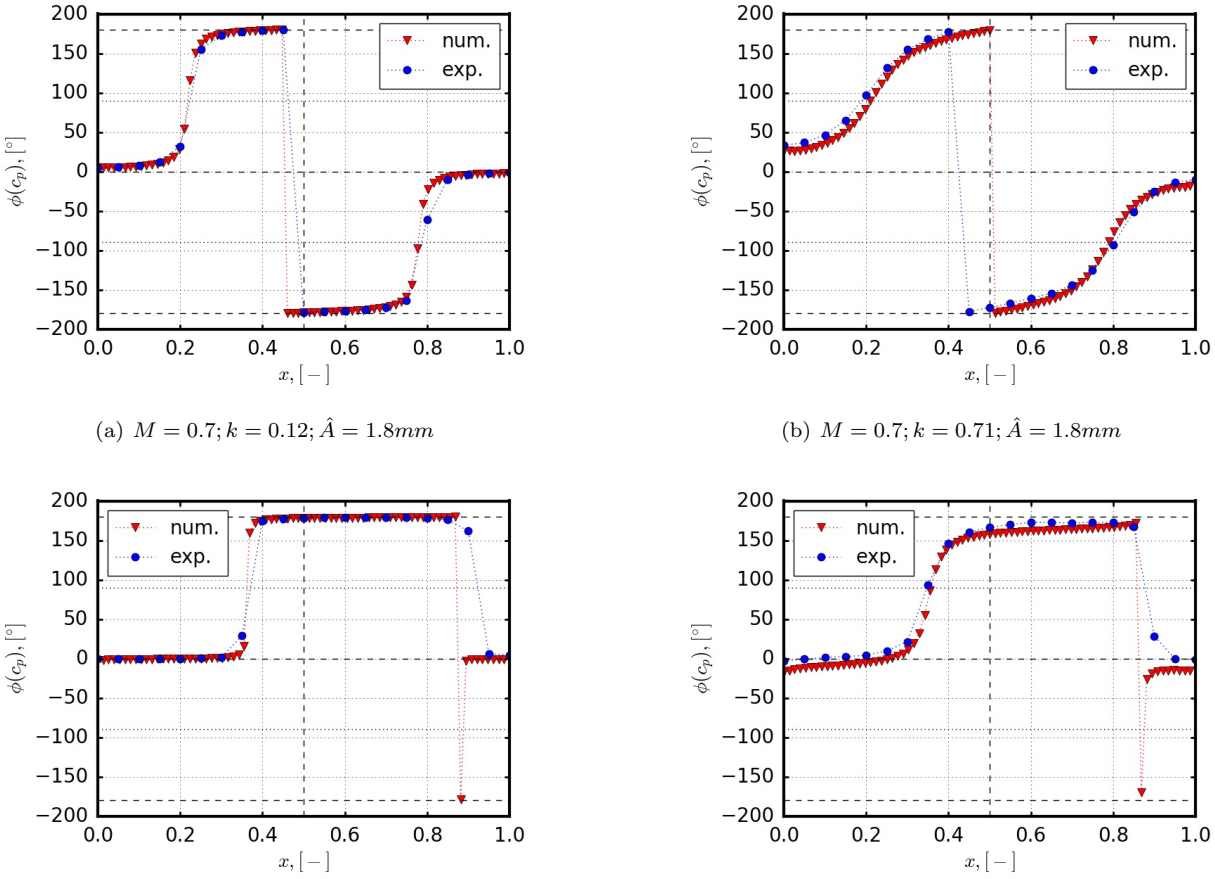

(a) $M = 0.7; k = 0.12; \hat{A} = 1.8mm$

(b) $M = 0.7; k = 0.71; \hat{A} = 1.8mm$

(c) $M = 1.15; k = 0.07; \hat{A} = 1.8mm$

(d) $M = 1.15; k = 0.51; \hat{A} = 1.8mm$

Figure 11. Pressure distribution, Comparison of phase angles.

domains of energy transfer between structure and fluid shall give further information on aeroelastic instability. For a completion of the needed data for the aeroelastic behaviour of panels further experiments are scheduled for spring 2017. Here the second bending mode shape is the design shape for the forced motion experiment.

Acknowledgments

The work presented in the report on hand was done within a cooperation of the DLR Institute of Aeroelasticity, DLR Institute of Aerodynamics and Flow Technology and Airbus DS. Thanks go to TWG crew of the German-Dutch Wind Tunnels (DNW) and of the DLR Institute of Aeroelasticity. Further thanks go to Bernhard Kotzias, Peter Nding and Martin Konopka from Airbus DS for the support.

References

[1]Garrick, I. E. and Reed III, Wilmer H., "Historical Development of Aircraft Flutter," *Journal of Aircraft*, Vol. 18, No. 11, 1981, pp. 897–912.

[2]Dowell, E. H., *Aeroelasticity of plates and shells*, Monographs and textbooks on mechanics of solids and fluids, Noordhoff International, Leyden, 1975.

[3]Dowell, E. H. and Bendiksen, O., "Panel Flutter," *Encyclopedia of Aerospace Engineering*, 2010.

[4]Johns, D. J., *A Survey on Panel Flutter*, AGARD Advisory Rept. 1, 1965.

[5]Muhlstein, L., Gaspers, P. A., and Riddle, D. W., *An experimental study of the influence of the turbulent boundary layer on panel flutter*, Vol. 4486 of *NASA technical note D*, National Aeronautics and Space Administration, Washington, DC, 1968.

[6]Gaspers, P. A., Muhlstein, L., and Petroff, D. N., *Further experimental results on the influence of the turbulent boundary layer on panel flutter*, Vol. 5798 of *NASA technical note D*, National Aeronautics and Space Administration, Washington, DC, 1970.

[7]Fung, Y.-C., "Some Recent Contributions to Panel Flutter Research," *AIAA Journal*, Vol. 1, No. 4, 1963, pp. 898–909.

[8]Zeydel, E. F. E., "Study of the Pressure Distribution on Oscillating Panels in Low Supersonic Flow with Turbulent Boundary Layer," .

[9]Dowell, E. H., "Generalized Aerodynamic Forces on a Flexible Plate Undergoing Transient Motion in a Shear Flow with an Application to Panel Flutter," *AIAA 8th Aerospace Sciences Meeting*, 1970.

[10]Dowell, E. H., "Aerodynamic Boundary Layer Effects on Flutter and Damping of Plates," *Journal of Aircraft*, Vol. 10, No. 12, 1973, pp. 734–738.

[11]Hashimoto, A., Aoyama, T., and Nakamura, Y., "Effects of Turbulent Boundary Layer on Panel Flutter," *AIAA Journal*, Vol. 47, No. 12, 2009, pp. 2785–2791.

[12]Shishaeva, A., Vedeneev, V. V., and Aksenov, A., "Nonlinear single-mode and multi-mode panel flutter oscillations at low supersonic speeds," *Journal of Fluids and Structures*, Vol. 56, 2015, pp. 205–223.

[13]Alder, M., "Development and Validation of a Fluid–Structure Solver for Transonic Panel Flutter," *AIAA Journal*, 2015, pp. 1–13.

[14]Perkins, T. M., "Flutter Test of an Array of Full-Scale Panels from the Saturn S-IVB Stage at Transonic Mach numbers," .

[15]Vedeneev, V. V., Guvernyuk, S. V., Zubkov, A. F., and Kolotnikov, M. E., "Experimental observation of single-mode panel flutter in a supersonic gas flow," *Doklady Physics*, Vol. 54, No. 8, 2009, pp. 389–391.

[16]Muhlstein, L., "A forced-vibration technique for investigation of panel flutter," *2nd Aerodynamic Testing Conference*, 1966.

[17]Lebker, J., Alder, M., and Fink, H., "DESIGN AND INITIAL RUN OF A NEW TEST SETUP FOR INVESTIGATIONS ON THE AEROELASTIC STABILITY OF PANELS IN THE TRANSONIC MACH DOMAIN," 2016.